

Correlation and Lead-Lag Relationships in a Hawkes Microstructure Model

José Da Fonseca ^{*} Riadh Zaatour [†]

March 12, 2016

Abstract

The aim of this paper is to develop a multi-asset model based on the Hawkes process describing the evolution of assets at high frequency and to study the lead-lag relationship as well as the correlation between the stocks within this framework. Thanks to its strong analytical tractability several statistical quantities are explicitly computed and give some insight on the impact of the model parameters on these quantities. Furthermore, we compute the covariance matrix associated with the diffusive limit of the model so that the relation between the parameters driving the asset at high and low frequencies is explicit. We illustrate our results using index futures and stocks quoted in the Eurex market. The model can capture the existing lead-lag relationship between the assets.

JEL Classification: C13, C32, C58.

Keywords: Hawkes process, Lead-Lag relationship, Correlation, Diffusive limit.

^{*}Corresponding author: Auckland University of Technology, Business School, Department of Finance, Private Bag 92006, 1142 Auckland, New Zealand. Phone: ++64 9 9219999 extn 5063. Email: jose.dafonseca@aut.ac.nz

[†]Chair of Quantitative Finance, Ecole Centrale Paris, Grande Voie des Vignes, 92290 Châtenay-Malabry, France. Email: zaatour.riadh@yahoo.fr

1 Introduction

The interaction between stocks is an important aspect of financial theory. From optimal portfolio choice to basket option pricing one of the key ingredients is the modelling of the dependency between stocks. The correlation appears to be the natural mathematical concept to handle the interaction and in fact underlies many financial models. The correlation provides information on contemporaneous evolutions but in the markets this simultaneousness can be too stringent. A concept that relaxes this hypothesis is the lead-lag relationship which has also been extensively studied in the literature, among many others let us mention Herbst et al. (1987). More recently, the availability of high-frequency data also triggered research on this subject as the works of De Jong and Nijman (1997) and Huth and Abergel (2014) attest.

The purpose of this work is to develop a multi-asset model for stocks based on the Hawkes process and to study the correlation and lead-lag relationship within this framework. The model specifies the high-frequency dynamic for the stocks and heavily relies on the single-stock dynamic model proposed by Bacry et al. (2013a) and further extended to the multi-asset case in Bacry et al. (2013b). In the particular case of exponential kernel for the Hawkes process, initially proposed by Hawkes (1971) which allows for very explicit computations, we develop a model for which many of the statistical properties of the stocks can be computed¹. The model displays clustering and/or mean reversion behavior for the stock volatilities as in Da Fonseca and Zaatour (2015). Using the theoretical results of Bacry et al. (2013b) we compute the diffusive limit for the stocks thereby connecting the model driving the assets at high frequency with the covariance matrix driving the assets at low frequency (i.e. daily)². Within this framework we analyze the correlation as well as the lead-lag relationship between the stocks and provide some expansions to better understand the impact of model parameters on different financial quantities. We also compute the limit behavior associated with the dynamic. Here also the analytical results prove to be essential and such analysis cannot be performed within the frameworks

¹For earlier application of the Hawkes process see Hewlett (2006), Large (2007) and Bowsher (2007) among others. For a Hawkes process with general kernel see Bacry et al. (2012). Note that the use of the Hawkes process in the set of works developed in Bacry and Muzy (2014a); Bacry et al. (2012, 2013a,b) differs substantially from the previous ones, which essentially used the likelihood function available in closed form for this process, by developing analytical aspects that open a wide range of applications.

²The problem of connecting the dynamics for the stocks at different time scales appears recently in several works. Without being exhaustive let us mention Cont and De Larrard (2012), Bacry et al. (2013a), Bacry et al. (2013b), Abergel and Jedidi (2013), Jedidi and Abergel (2013), Kirilenko et al. (2013). This aspect heavily relies on the analytical results.

previously used³. We then perform an empirical analysis on two index futures and four major stocks quoted on the Eurex market to illustrate the model. As expected, we find that the major index futures leads all the other assets (either stocks or “smaller” index futures). Between two similar assets (i.e. two stocks) the lead-lag relationship is time varying and when averaged over a long period no stock systematically leads the others. In a very particular case where one of the stock leads the other, the shareholder structure provides a reasonable explanation. Lastly, within our framework extracting a lead-lag relationship between stocks at low frequency is problematic and confirms the results of Huth and Abergel (2014).

The structure of the paper is as follows. In the first section, we describe the analytical framework which comprises the basic properties of the Hawkes process as well as the Dynkin formula that allows the computation of the moments and the autocorrelation function of the number of jumps over a given time interval. In the second section, given a dynamic for two stocks based on the Hawkes process, we derive various statistical quantities as well as the expression for the diffusive limit associated with the two stocks. We also make explicit how shocks propagate between the two assets and we perform some Taylor expansion that allow us to clarify the impact of parameters on the financial quantities. In the third section, an empirical analysis is performed to illustrate the capabilities of the model. Finally, we conclude and collate some technical results, tables and figures in the appendix.

2 Mathematical Framework

2.1 The multivariate Hawkes process

Let $X_t = (\lambda_t, N_t)$ is a Markov process in the state space $D = \mathbb{R}_+^n \times \mathbb{N}^n$, which satisfies the dynamic:

$$d\lambda_t = \beta(\lambda_\infty - \lambda_t)dt + \alpha dN_t \quad (1)$$

with β, α two $n \times n$ real matrices and λ_∞ a vector of \mathbb{R}^n . Applying Ito’s lemma to $e^{\beta t} \lambda_t$ yields:

$$\lambda_t = e^{-\beta t} (\lambda_0 - \lambda_\infty) + \lambda_\infty + \int_0^t e^{-\beta(t-v)} \alpha dN_v. \quad (2)$$

From Eq.(2) and under the hypothesis that β has positive eigenvalues we observe that the impact on the intensity of a jump dies out exponentially as time passes. Also, as the intensities must be positive

³The frameworks we are referring to are those used in Chan (1992), De Jong and Nijman (1997), De Jong and Donders (1998) or Frino et al. (2000) for example.

we deduce that the matrix α has to be component-wise positive. For the existence and uniqueness results we refer to Chapter 14 of Daley and Jones (2008) and references therein as well as Brémaud and Massoulié (1994) which is of particular interest.

As t gets larger the impact of λ_0 , the initial value for the intensity, vanishes leaving us with:

$$\lambda_t \sim \lambda_\infty + \int_0^t e^{-\beta(t-v)} \alpha dN_v.$$

Our presentation differs slightly from the usual one found in the literature where the Hawkes intensity is written as:

$$\lambda_t = \lambda_\infty + \int_{-\infty}^t e^{-\beta(t-v)} \alpha dN_v. \quad (3)$$

The Eq.(3) leads to a stochastic differential equation similar to Eq.(1), the process starts infinitely in the past and is at its stationary regime. In our case we have a dependency with respect to the initial position λ_0 in Eq.(2) but, as mentioned above, as t gets larger its impact vanishes.

Our presentation for the Hawkes process follows closely Errais et al. (2010) and is motivated by the fact that we want to perform stochastic differential calculus.

The infinitesimal generator of the diffusion is given by

$$\mathcal{L}f = (\beta(\lambda_\infty - \lambda))^\top \nabla^\top f + \lambda^\top \begin{pmatrix} f(\lambda + \alpha e_1, N_t + e_1) - f \\ \cdots \\ \cdots \\ f(\lambda + \alpha e_n, N_t + e_n) - f \end{pmatrix} \quad (4)$$

for $f : D \rightarrow \mathbb{R}$, where $\nabla f = (\partial_{\lambda_1} f, \dots, \partial_{\lambda_n} f)$ is a $1 \times n$ vector and $(e_i)_{i=1..n}$ is the canonical basis of \mathbb{R}^n (\top stands for the matrix transpose). For every function f in the domain of the infinitesimal generator, the process:

$$M_t = f(X_t) - f(X_0) - \int_0^t \mathcal{L}f(X_v) dv$$

is a martingale relative to its natural filtration (see for example Proposition 1.6 of chapter VII in Revuz and Yor (1999)) and for $s > t$ we have:

$$\mathbb{E} \left[f(X_s) - \int_0^s \mathcal{L}f(X_v) dv | \mathcal{F}_t \right] = f(X_t) + \int_t^s \mathcal{L}f(v, X_v) dv$$

by the martingale property, so finally:

$$\mathbb{E}[f(X_s)|\mathcal{F}_t] = f(X_t) + \mathbb{E}\left[\int_t^s \mathcal{L}f(X_v) dv|\mathcal{F}_t\right]. \quad (5)$$

This gives a very convenient way to calculate conditional expectations of functions of the Markov process $X_t = (\lambda_t, N_t)$ when the expectation of the right hand side of the preceding equation can be easily computed.

Notice also that taking the expectation of the above formula turns the conditional expectation into an unconditional expectation of quantities depending on the process (λ_t, N_t) .

The infinitesimal generator of the diffusion leads, thanks to Feynman-Kac's formula, to the computation of the moment-generating function. Denoted by $\phi(t, z, u) = \mathbb{E}\left[e^{z^\top \lambda_t + u^\top N_t}\right]$ for $z \in \mathbb{R}^n$ and $u \in \mathbb{N}^n$, this function solves the partial differential equation with initial condition:

$$\begin{cases} \partial_t \phi = \mathcal{L}\phi \\ \phi(0, z, u) = e^{z^\top \lambda_0 + u^\top N_0}. \end{cases}$$

The model being affine we look for a solution of the form $e^{a_t + b_t^\top \lambda + u^\top N}$ with $a_t \in \mathbb{R}$ and $b_t \in \mathbb{R}^n$. It leads to a set of ordinary differential equations:

$$\begin{cases} \partial_t a = b^\top \beta \lambda_\infty \\ \partial_t b = -\beta^\top b + h - \mathbf{1} \end{cases}$$

with initial conditions $a_0 = 0$, $b_0 = z$, and $\mathbf{1} = (1, \dots, 1)^\top$ while the function h is defined as:

$$h = \begin{pmatrix} e^{b^\top \alpha e_1 + u^\top e_1} \\ \dots \\ e^{b^\top \alpha e_n + u^\top e_n} \end{pmatrix}.$$

From a numerical point of view it is always possible to simulate the ordinary differential equations (ODE) but explicitly computing the solution is difficult. Also, if we are interested in the moments of the process then we need to derive the solution with respect to the parameter z which in turn leads to the computation of the derivative with respect to this parameter of the ODE. Although the first moment can be easily computed, higher moments remain a challenge. To the extent that we are interested only in the moments we can devise a simpler computation strategy based on Dynkin's formula given by Eq.(5).

2.2 The moments and autocorrelation function

We report in this section the expression for the moments of the process $X_t = (\lambda_t, N_t)$ and also the autocovariance of the number of jumps over a period τ . These results heavily rely on the use of the infinitesimal generator of the process given by Eq.(4) and Dynkin's formula Eq.(5). To make the document self-contained we report in the appendix a sketch of the proofs for the following results (see also Da Fonseca and Zaatour (2014) and Da Fonseca and Zaatour (2015)). We refer to Errais et al. (2010), Aït-Sahalia et al., Bacry et al. (2013a), Bacry et al. (2013b) and Bacry and Muzy (2014b) for other (and sometimes very elegant) results with the two last papers providing a very general case. Note that in these latter works when it comes to explicit computations the form of the kernel is different from ours⁴. In order to obtain the expected number of jumps and the expected intensity we use the following lemma.

Lemma 1 *Given a Hawkes process $X_t = (\lambda_t, N_t)$ with dynamic given by Eq.(1) then the expected number of jumps $\mathbb{E}[N_t]$ and the expected intensity $\mathbb{E}[\lambda_t]$ satisfy the set of ODE:*

$$d\mathbb{E}[\lambda_t] = \beta(\lambda_\infty - \mathbb{E}[\lambda_t])dt + \alpha\mathbb{E}[\lambda_t]dt, \quad (6)$$

$$d\mathbb{E}[N_t] = \mathbb{E}[\lambda_t]dt. \quad (7)$$

These equations can be integrated explicitly as we have:

$$\mathbb{E}[\lambda_t] = (\alpha - \beta)^{-1} \left(e^{(\alpha-\beta)t} - I \right) \beta\lambda_\infty + e^{(\alpha-\beta)t} \lambda_0 \quad (8)$$

$$= c_0(t)\lambda_0 + c_1(t) \quad (9)$$

and

$$\begin{aligned} \mathbb{E}[N_t] &= N_0 + (\alpha - \beta)^{-1} \left(e^{(\alpha-\beta)t} - I \right) \lambda_0 + \left(((\alpha - \beta)^{-1})^2 \left(e^{(\alpha-\beta)t} - I \right) \beta\lambda_\infty - (\alpha - \beta)^{-1} \beta\lambda_\infty t \right) \\ &= N_0 + c_2(t)\lambda_0 + c_3(t). \end{aligned} \quad (10)$$

Thanks to these two solutions we can compute the following asymptotic expectations.

Lemma 2 *Given a Hawkes process with dynamic given by Eq.(1) then long term expected intensity is given by:*

$$\lim_{t \rightarrow +\infty} \mathbb{E}[\lambda_t] = \bar{\lambda}_\infty = -(\alpha - \beta)^{-1} \beta\lambda_\infty \quad (11)$$

⁴The kernel is the function involved in the integral in Eq.(2). In our case it is of exponential form and constitutes the classical Hawkes process as initially defined by Hawkes (1971), it allows us to derive some explicit computations. More general kernels are possible but can come with a lack of analytical tractability.

whereas the long term expected number of jumps over an interval τ is:

$$\lim_{t \rightarrow +\infty} \mathbb{E}[N_{t+\tau} - N_t] = -(\alpha - \beta)^{-1} \beta \lambda_\infty \tau \quad (12)$$

$$= \bar{\lambda}_\infty \tau. \quad (13)$$

Establishing Eq.(11) requires that $\alpha - \beta$ has negative eigenvalues and is the classical stability condition of the multivariate Hawkes Process as stated in Hawkes (1971). Therefore, from now on we will suppose this property satisfied. We are interested in asymptotic values because in the applications developed in this paper the variable N_t will be observable but not the intensity λ_t . As a result, any time t conditional expectation of the process $N_{t+\tau}$ will depend, a priori, on λ_t and to simplify this dependency with respect to this unobservable variable we set the process to its long term value (by taking the limit for $t \rightarrow +\infty$). This astute strategy, used in Bacry et al. (2013a) or Aït-Sahalia et al., eases significantly the applications. The computation of the second order moments leads to the following lemma.

Lemma 3 *Given a Hawkes process $X_t = (\lambda_t, N_t)$ with dynamic given by Eq.(1) then the functions $\mathbb{E}[N_t N_t^\top]$, $\mathbb{E}[\lambda_t N_t^\top]$ and $\mathbb{E}[\lambda_t \lambda_t^\top]$ solve the set of ODE:*

$$\frac{d}{dt} \mathbb{E}[N_t N_t^\top] = \mathbb{E}[\lambda_t N_t^\top] + \mathbb{E}[N_t \lambda_t^\top] + \text{diag}(\mathbb{E}[\lambda_t]), \quad (14)$$

$$\frac{d}{dt} \mathbb{E}[\lambda_t N_t^\top] = \beta \lambda_\infty \mathbb{E}[N_t^\top] + (\alpha - \beta) \mathbb{E}[\lambda_t N_t^\top] + \mathbb{E}[\lambda_t \lambda_t^\top] + \alpha \text{diag}(\mathbb{E}[\lambda_t]), \quad (15)$$

$$\frac{d}{dt} \mathbb{E}[\lambda_t \lambda_t^\top] = \beta \lambda_\infty \mathbb{E}[\lambda_t^\top] + \mathbb{E}[\lambda_t] \lambda_\infty^\top \beta^\top + (\alpha - \beta) \mathbb{E}[\lambda_t \lambda_t^\top] + \mathbb{E}[\lambda_t \lambda_t^\top] (\alpha - \beta)^\top + \alpha \text{diag}(\mathbb{E}[\lambda_t]) \alpha^\top \quad (16)$$

and the long term covariance matrix for the intensity $\Lambda_\infty = \lim_{t \rightarrow +\infty} \mathbb{E}[\lambda_t \lambda_t^\top]$ solves the algebraic matrix equation:

$$(\alpha - \beta) \bar{\Lambda}_\infty + \bar{\Lambda}_\infty (\alpha - \beta)^\top + \alpha \text{diag}(\bar{\lambda}_\infty) \alpha^\top = 0 \quad (17)$$

with $\bar{\Lambda}_\infty = \Lambda_\infty - \bar{\lambda}_\infty \bar{\lambda}_\infty^\top$ where $\bar{\lambda}_\infty$ is given by Eq.(11).

Using the previous lemmas we can compute the second order moment as well as the auto-covariance function of the number of jumps over a given time interval. We refer to Da Fonseca and Zaatour (2015) for more details. We start with the next lemma.

Lemma 4 *The long term second order moment of the number of jumps over a given interval $\tau > 0$ is:*

$$\begin{aligned}\text{Cov}(\tau) &= \lim_{t \rightarrow +\infty} \mathbb{E} \left[(N_{t+\tau} - N_t)(N_{t+\tau} - N_t)^\top \right] - \mathbb{E}[(N_{t+\tau} - N_t)] \mathbb{E} \left[(N_{t+\tau} - N_t)^\top \right] \\ &= J_1 + J_1^\top + \tau \text{diag}(\bar{\lambda}_\infty)\end{aligned}\tag{18}$$

with $J_1 = c_5(\tau)(\bar{\Lambda}_\infty + \alpha \text{diag}(\bar{\lambda}_\infty))$ and

$$c_5(\tau) = -(\alpha - \beta)^{-1}\tau + (\alpha - \beta)^{-2}(e^{(\alpha-\beta)\tau} - I).\tag{19}$$

As we are interested in the autocorrelation structure of the process the following quantity proves to be essential.

Lemma 5 *Given $t_1 < t_2 \leq t_3 < t_4$ with $t_2 - t_1 = \tau_1$, $t_4 - t_3 = \tau_2$ and $t_3 - t_2 = \delta$ we have:*

$$\begin{aligned}\text{Cov}_1(\tau_1, \tau_2, \delta) &= \lim_{t_1 \rightarrow +\infty} \mathbb{E} \left[(N_{t_4} - N_{t_3})(N_{t_2} - N_{t_1})^\top \right] - \mathbb{E}[(N_{t_4} - N_{t_3})] \mathbb{E} \left[(N_{t_2} - N_{t_1})^\top \right] \\ &= c_2(\tau_2)c_0(\delta)c_2(\tau_1) (\bar{\Lambda}_\infty + \alpha \text{diag}(\bar{\lambda}_\infty))\end{aligned}\tag{20}$$

with $\bar{\Lambda}_\infty$ given by Eq.(17) and $\bar{\lambda}_\infty$ by Eq.(11).

It is possible to relax the assumption of overlapping intervals made in the previous lemma as the next result shows.

Lemma 6 *Given $t_1 < t_3 \leq t_2 < t_4$ with $t_2 - t_1 = \tau_1$, $t_4 - t_3 = \tau_2$ and $t_3 - t_1 = \delta$ (note the difference with the previous lemma), then:*

$$\begin{aligned}\text{Cov}_2(\tau_1, \tau_2, \delta) &= \lim_{t_1 \rightarrow +\infty} \mathbb{E} \left[(N_{t_4} - N_{t_3})(N_{t_2} - N_{t_1})^\top \right] - \mathbb{E}[N_{t_4} - N_{t_3}] \mathbb{E} \left[(N_{t_2} - N_{t_1})^\top \right] \\ &= \text{Cov}_1(\tau_1, \tau_2 - (\tau_1 - \delta), 0) + \text{Cov}(\tau_1 - \delta) + \text{Cov}_1(\delta, \tau_1 - \delta, 0).\end{aligned}\tag{21}$$

The expression for the autocovariance function leads naturally to the autocorrelation function of the number of jumps over a given time interval denoted as $\text{CORR}(\tau, \delta)$ which is a function of:

$$\lim_{t \rightarrow +\infty} \mathbb{E} \left[(N_{t+\tau} - N_t)(N_{t+\tau+\delta} - N_{t+\delta})^\top \right] - \mathbb{E}[N_{t+\tau} - N_t] \mathbb{E} \left[(N_{t+\tau+\delta} - N_{t+\delta})^\top \right]\tag{22}$$

where, depending whether $\delta \geq \tau$ or not, we use either Eq.(20) or Eq.(21) and the square root of the diagonal terms of the matrices $\text{Cov}(\tau)$. Lemma 5 leads to the following useful result whose proof is straightforward and thus omitted.

Lemma 7 *Given the covariance matrix $\text{COV}_1(\tau_1, \tau_2, \delta)$ defined by Eq.(20) then we have:*

$$\begin{aligned}\bar{\Sigma} &= \sum_{j=0}^{\infty} \text{COV}_1(1, 1, j) \\ &= (\alpha - \beta)^{-2} (I - e^{\alpha - \beta})(\bar{\Lambda}_{\infty} + \alpha \text{diag}(\bar{\lambda}_{\infty})).\end{aligned}\tag{23}$$

Lastly, the next lemma eases significantly the computation.

Lemma 8 *We suppose a four-dimensional Hawkes process $X_t = (\lambda_t, N_t)$ with values in $D = \mathbb{R}_+^4 \times \mathbb{N}^4$. Given the matrix $\bar{\Sigma}$ of Eq.(23), the covariance matrix $\text{COV}(1)$ defined by Eq.(18) and define $M = \text{COV}(1) + 2\bar{\Sigma}$ then:*

$$M_{11} + M_{22} - M_{12} - M_{21} = \tilde{M}_{11} + \tilde{M}_{22} - \tilde{M}_{12} - \tilde{M}_{21},\tag{24}$$

$$M_{33} + M_{44} - M_{34} - M_{43} = \tilde{M}_{33} + \tilde{M}_{44} - \tilde{M}_{34} - \tilde{M}_{43}\tag{25}$$

with:

$$\tilde{M} = \tilde{J}_1 + \tilde{J}_1^{\top} + \text{diag}(\bar{\lambda}_{\infty}),\tag{26}$$

$$\tilde{J}_1 = -(\alpha - \beta)^{-1}(\bar{\Lambda}_{\infty} + \alpha \text{diag}(\bar{\lambda}_{\infty})).\tag{27}$$

The numerical consequences of the previous lemma are important because the left hand side of Eq.(24) (or Eq.(25)) involves exponential of matrices, through c_5 of Lemma 4, whereas the right hand side involves no exponentiation.

These lemmas provide the main equations that will be involved in the applications developed in this paper.

3 The Bacry-Delattre-Hoffmann-Muzy Model

3.1 The stock dynamics

We adopt the modelling framework proposed by Bacry, Delattre, Hoffmann, and Muzy (2013a) to describe the evolution of the *mid* price of two traded assets:

$$\begin{aligned}S_t^1 &= S_0^1 + \left(N_t^{1,u} - N_t^{1,d}\right) \frac{\nu_1}{2}, \\ S_t^2 &= S_0^2 + \left(N_t^{2,u} - N_t^{2,d}\right) \frac{\nu_2}{2}\end{aligned}$$

where ν_1 and ν_2 are the tick values for the first stock and second stock, respectively. Let, $N_t^{1,u}$ and $N_t^{1,d}$ be Hawkes processes capturing the up and down jumps of the mid price for the first stock and $N_t^{2,u}$ and $N_t^{2,d}$ the corresponding equivalent for the second stock.

In this work the four dimensional Hawkes process $N_t = (N_t^{1,u}, N_t^{1,d}, N_t^{2,u}, N_t^{2,d})^\top$ and $\lambda_t = (\lambda_t^{1,u}, \lambda_t^{1,d}, \lambda_t^{2,u}, \lambda_t^{2,d})^\top$ follow a dynamic of the form Eq.(1) with:

$$\alpha = \begin{pmatrix} \alpha_s^1 & \alpha_m^1 & x & 0 \\ \alpha_m^1 & \alpha_s^1 & 0 & x \\ y & 0 & \alpha_s^2 & \alpha_m^2 \\ 0 & y & \alpha_m^2 & \alpha_s^2 \end{pmatrix}; \beta = \begin{pmatrix} \bar{\beta}_1 & 0 & 0 & 0 \\ 0 & \bar{\beta}_1 & 0 & 0 \\ 0 & 0 & \bar{\beta}_2 & 0 \\ 0 & 0 & 0 & \bar{\beta}_2 \end{pmatrix} \quad (28)$$

and $\lambda_\infty = (\lambda_{1,\infty}, \lambda_{1,\infty}, \lambda_{2,\infty}, \lambda_{2,\infty})^\top \in \mathbb{R}_+^4$.

The connection between the two stocks is controlled through the 2×2 upper-right and lower-left submatrices (called coupling submatrices in the sequel). Our parametrization is compatible with two stocks with positive correlation and if $x = y = 0$ then the two stocks move independently.

As $x > 0$, an up move of the second stock, through a jump of $N_t^{2,u}$, induces an increase of the intensity $\lambda_t^{1,u}$ which increases the probability of a jump of $N_t^{1,u}$ over the next time period and therefore an up move of the first stock. Similar reasoning applies to a down move. As a consequence, the movements of the second stock will be reproduced by the first stock. By construction these related evolutions are *not simultaneous*, and produce a lead-lag relationship when observed at the adequate time scale. In the specific case where $x > 0$ and $y = 0$, the second asset leads the first asset and we can qualify as a positive lead-lag relationship, as the stocks will move in the same direction and their overall correlation will be positive.

We restrict ourselves to a very particular form for the coupling submatrices in order to make explicit, as much as possible the dependency between the stocks. For example, the 2×2 upper-right matrix of α could be replaced with:

$$\begin{pmatrix} x_1 & 0 \\ 0 & x_2 \end{pmatrix}, \quad (29)$$

then the impact of an up move of the second stock on the first one will be different from the impact

of a down move (of the second asset on the first asset). A priori this is an appealing feature because linkages between stocks are indeed different in bear and bull markets. However, to keep the analytical expressions simple we restrict this study to the symmetric model (i.e. $x_1 = x_2$).

If we wish to consider a negative lead-lag relationship of the second stock on the first one, that is to say a resulting negative correlation, then the 2×2 upper-right submatrix of α should be:

$$\begin{pmatrix} 0 & x \\ x & 0 \end{pmatrix}, \quad (30)$$

also with the possibility to differentiate up and down moves.

Similar considerations apply to 2×2 lower-left submatrix of α that controls the transmission of the shocks affecting the first stock to the second stock. Also, it is worth underlining the possibility of dissymmetric effects between the two stocks in the sense that the impact of the first stock on the second one need not to be equal, nor in the same direction, to the impact of the second stock on the first one. This strongly contrasts with the usual correlation which by definition is a reflexive relation. Although the model allows for a dissymmetric relationship between the stocks it seems to us natural to choose the upper-right matrix consistently with the lower-left matrix. For the choice made for the 2×2 upper-right matrix of α in Eq.(28) the natural choice is the one made for the lower-left sub-matrix whereas in the case of Eq.(30) then the natural choice is:

$$\begin{pmatrix} 0 & y \\ y & 0 \end{pmatrix}. \quad (31)$$

It would even be tempting to choose $x = y$ so that the lead-lag relationship would be reflexive. However, there are some practical cases where allowing for some dissymmetry, that is to say different values for x and y , is particularly relevant; the most well-known example being the relation between a futures on an index and a stock.

Following Bacry et al. (2013a) we will be interested in the diffusive limit for $S_t = (S_t^1, S_t^2)^\top$ associated with the dynamics Eq.(28). In order to perform such a limit computation the matrices α and β in Eq.(28) are such that $\mathbb{E}[N_t^{1,u}] = \mathbb{E}[N_t^{1,d}] = \mathbb{E}[N_t^{2,u}] = \mathbb{E}[N_t^{2,d}]$, this ensures the martingale property for the stocks. This martingale property can be obtained for more general matrices α and β but we

restrict this study to these particular forms to keep the expressions simple.

Thanks to the computations made above we know that the matrix $\alpha - \beta$ must have negative eigenvalues for the multivariate Hawkes process to be stable, which translates to:

$$\gamma_1 + \gamma_2 \pm \left((\gamma_1 + \gamma_2)^2 - 4(\gamma_1\gamma_2 - xy) \right)^{\frac{1}{2}} > 0, \quad (32)$$

$$\theta_1 + \theta_2 \pm \left((\theta_1 + \theta_2)^2 - 4(\theta_1\theta_2 - xy) \right)^{\frac{1}{2}} > 0 \quad (33)$$

with $\gamma_i = \bar{\beta}_i + \alpha_m^i - \alpha_s^i$, $\theta_i = \bar{\beta}_i - \alpha_m^i - \alpha_s^i$ for $i \in \{1, 2\}$. Conditions ensuring these inequalities are $\gamma_1\gamma_2 > xy$ and $\theta_1\theta_2 > xy$ that, from now on, we presume satisfied.

3.2 Statistical properties

Having specified the dynamics for the stocks we focus on the computation of various statistical properties associated with the assets. The use of high-frequency data enables the computation of the realized volatility and the estimator, for data sampled using time intervals of length τ , is written as:

$$\begin{aligned} \hat{C}_1(\tau) &= \frac{1}{T} \sum_{n=0}^{T/\tau-1} (S_{(n+1)\tau}^1 - S_{n\tau}^1)^2 = \frac{1}{T} \sum_{n=0}^{T/\tau-1} \left((N_{(n+1)\tau}^{1,u} - N_{n\tau}^{1,u}) - (N_{(n+1)\tau}^{1,d} - N_{n\tau}^{1,d}) \right)^2 \frac{\nu_1^2}{4} \\ &= \frac{1}{T} \sum_{n=0}^{T/\tau-1} (N_{(n+1)\tau}^{1,u} - N_{n\tau}^{1,u})^2 \frac{\nu_1^2}{4} + \frac{1}{T} \sum_{n=0}^{T/\tau-1} (N_{(n+1)\tau}^{1,d} - N_{n\tau}^{1,d})^2 \frac{\nu_1^2}{4} \\ &\quad - 2 \frac{1}{T} \sum_{n=0}^{T/\tau-1} (N_{(n+1)\tau}^{1,u} - N_{n\tau}^{1,u}) (N_{(n+1)\tau}^{1,d} - N_{n\tau}^{1,d}) \frac{\nu_1^2}{4}. \end{aligned}$$

The mean signature plot, or more simply signature plot, is the expectation of the above quantity and is explicitly given.

Proposition 9 *The signature plot for the first asset $C_1(\tau) = \mathbb{E}[\hat{C}_1(\tau)]$ is:*

$$C_1(\tau) = \frac{\nu_1^2}{4\tau} (M_{11} + M_{22} - M_{12} - M_{21}) \quad (34)$$

where $M = \text{COV}(\tau)$ is the second moment matrix calculated in Lemma 4.

The volatility of the second stock is obtained by the same calculations:

$$C_2(\tau) = \frac{\nu_2^2}{4\tau} (M_{33} + M_{44} - M_{34} - M_{43}). \quad (35)$$

This kind of expression appears in Da Fonseca and Zaatour (2014) and Da Fonseca and Zaatour (2015) for a single-stock model and in a multi-asset setting for specific values for the parameters,

different from the choice made in this paper, it leads to an expression already available in Bacry et al. (2013a). As such, it remains interesting to calculate it within the multi-asset model proposed here to understand how the structure of the matrices Eq.(28) will affect the different statistical quantities. For instance, let S_t^1 be a stock and S_t^2 be an index future that captures the overall market evolution. We can then assess the part of stock volatility that can be explained by market activity through the coupling parameters x and y . We will make this more clear in the sequel.

As we deal with a multi-asset model, the covariance between the two stocks is the quantity of interest and can be obtained by the usual estimator:

$$\begin{aligned}\widehat{\text{CovS}}(\tau) &= \frac{1}{T} \sum_{n=0}^{T/\tau-1} (S_{(n+1)\tau}^1 - S_{n\tau}^1) (S_{(n+1)\tau}^2 - S_{n\tau}^2) \\ &= \frac{1}{T} \sum_{n=0}^{T/\tau-1} \left[\left(N_{(n+1)\tau}^{1,u} - N_{n\tau}^{1,u} \right) \left(N_{(n+1)\tau}^{2,u} - N_{n\tau}^{2,u} \right) - \left(N_{(n+1)\tau}^{1,u} - N_{n\tau}^{1,u} \right) \left(N_{(n+1)\tau}^{2,d} - N_{n\tau}^{2,d} \right) \right. \\ &\quad \left. - \left(N_{(n+1)\tau}^{1,d} - N_{n\tau}^{1,d} \right) \left(N_{(n+1)\tau}^{2,u} - N_{n\tau}^{2,u} \right) + \left(N_{(n+1)\tau}^{1,d} - N_{n\tau}^{1,d} \right) \left(N_{(n+1)\tau}^{2,d} - N_{n\tau}^{2,d} \right) \right] \frac{\nu_1 \nu_2}{4}.\end{aligned}$$

This estimator along with the analytical results, mainly the second moment of Lemma 4, lead to an explicit expression for the covariance as the following proposition shows.

Proposition 10 *The covariance between the two stocks implied by $\widehat{\text{CovS}}(\tau)$ is:*

$$\text{CovS}(\tau) = \frac{\nu_1 \nu_2}{4\tau} \left[M_{13} - M_{14} - M_{23} + M_{24} \right] = \frac{\nu_1 \nu_2}{4\tau} \left[M_{31} - M_{41} - M_{32} + M_{42} \right] \quad (36)$$

with the matrix $M = \text{Cov}(\tau)$ given by Eq.(18) of Lemma 4. The last equality in Eq.(36) stands from the symmetry of the matrix M .

Scaling the above equation by the stock volatilities one can obtain an estimator of the correlation as a function of the sampling period τ and retrieves the well-known Epps effect. This effect materializes the decrease of the estimated correlation when the sampling frequency increases. An illustration for this model is given in Figure 1.

[Insert Figure 1 here]

Beyond the correlation between the two stocks is the lead-lag relationship. The estimator of the lagged covariance between the two stocks if we consider S^2 as the leader is:

$$\begin{aligned}
\hat{L}_{2 \rightarrow 1}(\tau, \delta) &= \frac{1}{T} \sum_{n=0}^{T/\tau-1} (S_{(n+1)\tau+\delta}^1 - S_{n\tau+\delta}^1) (S_{(n+1)\tau}^2 - S_{n\tau}^2) \\
&= \frac{1}{T} \sum_{n=0}^{T/\tau-1} \left[\left(N_{(n+1)\tau+\delta}^{1,u} - N_{n\tau+\delta}^{1,u} \right) \left(N_{(n+1)\tau}^{2,u} - N_{n\tau}^{2,u} \right) - \left(N_{(n+1)\tau+\delta}^{1,u} - N_{n\tau+\delta}^{1,u} \right) \left(N_{(n+1)\tau}^{2,d} - N_{n\tau}^{2,d} \right) \right. \\
&\quad \left. - \left(N_{(n+1)\tau+\delta}^{1,d} - N_{n\tau+\delta}^{1,d} \right) \left(N_{(n+1)\tau}^{2,u} - N_{n\tau}^{2,u} \right) + \left(N_{(n+1)\tau+\delta}^{1,d} - N_{n\tau+\delta}^{1,d} \right) \left(N_{(n+1)\tau}^{2,d} - N_{n\tau}^{2,d} \right) \right] \frac{\nu_1 \nu_2}{4}.
\end{aligned}$$

for $\delta > 0$. Conversely, if the first stock is taken as the leader the estimator becomes:

$$\hat{L}_{1 \rightarrow 2}(\tau, \delta) = \frac{1}{T} \sum_{n=0}^{T/\tau-1} (S_{(n+1)\tau+\delta}^2 - S_{n\tau+\delta}^2) (S_{(n+1)\tau}^1 - S_{n\tau}^1).$$

These two estimators combined with the results developed in the analytical part give the following proposition.

Proposition 11 *Given the two estimators defined above then the estimated lagged covariances, depending on which asset is chosen as leader, write as:*

$$L_{2 \rightarrow 1}(\tau, \delta) = \frac{\nu_1 \nu_2}{4\tau} \left[\text{Cov}(\tau, \delta)_{13} - \text{Cov}(\tau, \delta)_{14} - \text{Cov}(\tau, \delta)_{23} + \text{Cov}(\tau, \delta)_{24} \right], \quad (37)$$

$$L_{1 \rightarrow 2}(\tau, \delta) = \frac{\nu_1 \nu_2}{4\tau} \left[\text{Cov}(\tau, \delta)_{31} - \text{Cov}(\tau, \delta)_{32} - \text{Cov}(\tau, \delta)_{41} + \text{Cov}(\tau, \delta)_{42} \right] \quad (38)$$

for $\tau > 0$ and $\delta > 0$ while $\text{Cov}(\tau, \delta)$ stands for $\text{Cov}_1(\tau, \tau, \delta)$ or $\text{Cov}_2(\tau, \tau, \delta)$ (these two quantities given by Eq.(20) and Eq.(21)) depending on how δ compares with τ .

From these two quantities we can define a lead-lag correlation between the two stocks for $(\tau, \delta) \in \mathbb{R}_+ \times \mathbb{R}$ as:

$$\mathcal{C}(\tau, \delta) = \begin{cases} \frac{L_{2 \rightarrow 1}(\tau, \delta)}{\sqrt{C_1(\tau)C_2(\tau)}} & \text{if } \delta > 0, \\ \frac{L_{1 \rightarrow 2}(\tau, -\delta)}{\sqrt{C_1(\tau)C_2(\tau)}} & \text{if } \delta < 0. \end{cases}$$

An illustration of the lagged correlation is given in Figure 2.

[Insert Figure 2 here]

Suppose that $x > 0$ and $y = 0$ then an up jump of the second asset will induce an increase of $\lambda_t^{1,u}$ which increases the probability of an up jump of the first asset will occur, if it occurs, with a delay. As a result, the function $\delta \rightarrow \mathcal{C}(\tau, \delta)$ should be increasing at the vicinity of 0_+ . Conversely, if $x = 0$ and

$y > 0$ then an up move of the first asset will imply an increase of $\lambda_t^{2,u}$ which increases the probability of an up jump of the second asset will occur, if it occurs, with a delay. In that case the function $\delta \rightarrow \mathcal{C}(\tau, \delta)$ will be decreasing at 0_- . Clearly, the function $\delta \rightarrow \mathcal{C}(\tau, \delta)$ should converge to zero for $|\delta|$ large and we expect a humped shape. If the effect provoked by x dominates then the maximum of $\delta \rightarrow \mathcal{C}(\tau, \delta)$ should be for $\delta > 0$, and in that case the second asset leads the first one; whereas if the y effect dominates we expect the opposite, that is to say, a maximum for δ negative and in that case the first asset is the leader. Lastly, the two effects can cancel each other and it leads to a centred function, none of the assets leads the other.

3.3 The diffusive limit behavior

In the previous section the dynamic is supposed to modelize the stock price evolution at high-frequency. At low frequency, typically daily, the usual framework is the one based on continuous diffusion processes driven by a Brownian motion. Recently, some works tried to fill the gap between these two time scales and these results are of interest because it enables the development of a micro foundation of daily quantities (the most well known being the Black-Scholes volatility). Along these lines let us mention, without pretending to be exhaustive, the works of Abergel and Jedidi (2013), Cont and De Larrard (2013), Cont and De Larrard (2012) and Kirilenko et al. (2013). For the models based on the Hawkes process most of the results, if not all, were systematically developed in Bacry et al. (2013a), Bacry et al. (2013b) and Bacry and Muzy (2014a). We follow these authors and focus on the diffusive limit associated with the model proposed here with the aim of underlining the impact of the parameters on the quantities driving the stock at low frequency.

In order to compute the diffusive limit of the model we use the important Corollary 1 of Bacry et al. (2013b) which gives a central limit theorem for the Hawkes process.

Proposition 12 *Let N_t the four-dimensional Hawkes process then for $t \in [0; 1]$*

$$\frac{N_{nt}}{\sqrt{n}} - \sqrt{nt}\bar{\lambda}_\infty \tag{39}$$

converge in law for the Skorohod topology to:

$$(\beta - \alpha)^{-1} \beta \Sigma^{\frac{1}{2}} W_t \tag{40}$$

with $\{W_t; t \geq 0\}$ a four-dimensional Brownian motion and Σ the diagonal matrix with the i^{th} element given by $((\beta - \alpha)^{-1} \beta \lambda_\infty)_i$.

Let us then write unit-time price increments for the first asset as similar results apply to the second asset:

$$\eta_i^1 = \left[(N_i^{1,u} - N_{i-1}^{1,u}) - (N_i^{1,d} - N_{i-1}^{1,d}) \right] \times \frac{\nu_1}{2},$$

and consider the random sums

$$S_n^1 = \sum_{i=1}^n \eta_i^1.$$

Denote by:

$$\bar{S}_t^{1,n} = \frac{S_{[nt]}^1}{\sqrt{n}},$$

and let $\bar{S}_t^n = (\bar{S}_t^{1,n}, \bar{S}_t^{2,n})^\top$ the vector of the two stocks. Thanks to Proposition 12 we obtain the diffusive limit for the stocks.

Proposition 13 *The vector \bar{S}_t^n converges in law to the vector $\tilde{S}_t = (\tilde{S}_t^1, \tilde{S}_t^2)^\top$ whose dynamic is given by:*

$$\begin{aligned} d\tilde{S}_t^1 &= \frac{\nu_1}{2} \sum_{j=1}^4 (m_{1j} - m_{2j}) dW_t^j, \\ d\tilde{S}_t^2 &= \frac{\nu_2}{2} \sum_{j=1}^4 (m_{3j} - m_{4j}) dW_t^j \end{aligned}$$

with m the matrix appearing in Eq.(40).

The stock price increments follow a Gaussian distribution, in the literature this model is usually referred to as the Bachelier model, from which we deduce the assets' covariance matrix.

Proposition 14 *Let the 2×2 covariance matrix of the assets such that:*

$$\sigma \sigma^\top = \begin{pmatrix} \sigma_{11}^2 & \sigma_{12} \\ \sigma_{12} & \sigma_{22}^2 \end{pmatrix}$$

then we have:

$$\sigma_{11}^2 = \frac{\nu_1^2}{4} \sum_{j=1}^4 (m_{1j} - m_{2j})^2, \quad (41)$$

$$\sigma_{12} = \frac{\nu_1 \nu_2}{4} \sum_{j=1}^4 (m_{1j} - m_{2j})(m_{3j} - m_{4j}), \quad (42)$$

$$\sigma_{22}^2 = \frac{\nu_2^2}{4} \sum_{j=1}^4 (m_{3j} - m_{4j})^2 \quad (43)$$

that are explicitly given by

$$\sigma_{11}^2 = \frac{\nu_1^2}{4} \frac{2\lambda_{1,\infty}(\bar{\beta}_1 \bar{\beta}_2^2 x^2 y + \bar{\beta}_1^3 \theta_2 \gamma_2^2) + \lambda_{2,\infty} \bar{\beta}_2 x (\bar{\beta}_2^2 x \theta_1 + \bar{\beta}_1^2 \gamma_2^2)}{(\gamma_1 \gamma_2 - xy)^2 (\theta_1 \theta_2 - xy)}, \quad (44)$$

$$\sigma_{12} = \frac{\nu_1 \nu_2}{4} \frac{2\bar{\beta}_1 y \lambda_{1,\infty}(\bar{\beta}_2^2 x \gamma_1 + \bar{\beta}_1^2 \theta_2 \gamma_2) + 2\bar{\beta}_2 x \lambda_{2,\infty}(\bar{\beta}_1^2 y \gamma_2 + \bar{\beta}_2^2 \theta_1 \gamma_1)}{(\gamma_1 \gamma_2 - xy)^2 (\theta_1 \theta_2 - xy)}, \quad (45)$$

$$\sigma_{22}^2 = \frac{\nu_2^2}{4} \frac{2\lambda_{2,\infty}(\bar{\beta}_2 \bar{\beta}_1^2 y^2 x + \bar{\beta}_2^3 \theta_1 \gamma_1^2) + \lambda_{1,\infty} \bar{\beta}_1 y (\bar{\beta}_1^2 y \theta_2 + \bar{\beta}_2^2 \gamma_1^2)}{(\gamma_1 \gamma_2 - xy)^2 (\theta_1 \theta_2 - xy)} \quad (46)$$

with $\gamma_i = \bar{\beta}^i + \alpha_m^i - \alpha_s^i$ and $\theta_i = \bar{\beta}^i - \alpha_m^i - \alpha_s^i$ $i \in \{1, 2\}$.

Remark 15 Note that when $x = y = 0$ then $\sigma_{12} = 0$ and $\sigma_{11}^2 = \frac{\nu_1^2}{2} \Lambda_1 \kappa_1^2$ as in Bacry et al. (2013a) if $\alpha_s^1 = 0$, or in Da Fonseca and Zaatour (2014) if $\alpha_m^1 = 0$, or Da Fonseca and Zaatour (2015) if $\alpha_s^1 \neq 0$ and $\alpha_m^1 \neq 0$.

Remark 16 From Proposition 9 we can retrieve the diffusive limit for the volatility by considering the limit $\lim_{\tau \rightarrow +\infty} C(\tau)$ in Eq.(34), it leads to the computation of $\lim_{\tau \rightarrow +\infty} \frac{1}{\tau} \text{Cov}(\tau)$ with $\text{Cov}(\tau)$ given by Eq.(18). Taking into account the form of $c_5(\tau)$ this limit is given by:

$$\lim_{\tau \rightarrow +\infty} \frac{1}{\tau} \text{Cov}(\tau) = \tilde{J}_1 + \tilde{J}_1^\top + \text{diag}(\bar{\Lambda}_\infty) \quad (47)$$

with $\tilde{J}_1 = -(\alpha - \beta)^{-1}(\bar{\Lambda}_\infty + \alpha \text{diag}(\bar{\Lambda}_\infty))$.

A similar remark applies to the covariance between the stocks given in Proposition 10, considering $\lim_{\tau \rightarrow +\infty} \text{CovS}(\tau)$ leads to the same limit equation.

Remark 17 Taking the limit with respect to τ in Eq.(37) and Eq.(38) gives $\lim_{\tau \rightarrow +\infty} L_{1,2}(\tau, \delta) = \lim_{\tau \rightarrow +\infty} L_{2,1}(\tau, \delta) = 0$. Thus, we cannot extract lead-lag relationship in the diffusive case or equivalently at low frequency (i.e. daily), a fact already underlined by Huth and Abergel (2014) and Bacry et al. (2013b). Note that this “flaw” is specific to our model and/or our approach. In Hoffmann et al.

(2013) a Bachelier model that allows for lead-lag relationship is proposed but the modelling strategy is completely different from ours.

From equation (45) we conclude that if $x = y = 0$ then $\sigma_{12} = 0$ is as expected. Due to sign constraints on the parameters if $x > 0$ and/or $y > 0$ we also conclude that $\sigma_{12} > 0$ is also consistent with the dynamic for the stocks. If in the matrix α of Eq.(28) the upper-right matrix is given by Eq.(30) and lower-left matrix is given by Eq.(31) then the volatilities σ_{11}^2 and σ_{22}^2 will still be given by Eq.(44) and Eq.(46) while the covariance σ_{12} will be minus the term Eq.(45). Hence, a negative correlation is achieved and it is consistent with the dynamic in that case.

3.4 Expansion with respect to coupling parameters

In order to gain some intuition on the impact of the model parameters we perform (first order) Taylor expansions of the computed quantities. As we are primarily interested in the interaction between the two stocks, the expansion will be done with respect to x and y that we qualify as coupling or lead-lag parameters. We first focus on the impact of the coupling parameters on the signature plot of the assets, the following proposition, which proof is postponed to the appendix, explains the dependency with respect to these parameters.

Proposition 18 *Given the signature plot for the first asset of Proposition 9 then we have the following first order Taylor expansion:*

$$C_1(\tau) = C_0(\tau) + xC_x(\tau) + yC_y(\tau) \quad (48)$$

where:

$$\begin{aligned} C_0(\tau) &= \frac{\nu_1^2}{2} \Lambda_1 \left(\kappa_1^2 + (1 - \kappa_1^2) \frac{(1 - e^{-\tau\gamma_1})}{\gamma_1\tau} \right), \\ C_x(\tau) &= \frac{\nu_1^2}{2} \frac{\Lambda_2}{\theta_1} \left(\kappa_1^2 + (1 - \kappa_1^2) \frac{(1 - e^{-\tau\gamma_1})}{\gamma_1\tau} \right), \\ C_y(\tau) &= 0 \end{aligned}$$

and

$$\Lambda_i = \frac{\bar{\beta}_i \lambda_{i,\infty}}{\theta_i}, \quad \kappa_i = \frac{\bar{\beta}_i}{\gamma_i}, \quad (49)$$

with θ_i and γ_i defined for $i \in \{1, 2\}$ were previously defined. A similar expression can be obtained for the second stock.

The expression of $C_0(\tau)$ appears in Bacry et al. (2013a) with the parameters computed under the hypothesis $\alpha_s^1 = 0$, or in Da Fonseca and Zaatour (2014) with the parameters computed under the hypothesis $\alpha_m^1 = 0$, or Da Fonseca and Zaatour (2015) with $\alpha_s^1 \neq 0$ and $\alpha_m^1 \neq 0$. Note that $C_y(\tau) = 0$. Of importance is the fact that the functions $\tau \rightarrow C_0(\tau)$ and $\tau \rightarrow C_x(\tau)$ have the same shape which implies that the coupling parameter does not alter the shape of the signature plot. It will be decreasing in the purely mutually excited case, i.e. $\alpha_s^1 = 0$ as in Bacry et al. (2013a), or increasing as in Da Fonseca and Zaatour (2014), or could be even flat if $\alpha_s^1 = \alpha_m^1$.

Having computed the expansion of the signature plot, using similar computations (we omit the proof) we can obtain the expansion for the covariance.

Proposition 19 *The covariance between two stocks of equation (36) has the Taylor expansion:*

$$\text{Cov}(\tau) = \frac{\nu_1 \nu_2}{4} (\text{Cov}_0(\tau) + x \text{Cov}_x(\tau) + y \text{Cov}_y(\tau)) \quad (50)$$

where:

$$\begin{aligned} \text{Cov}_0(\tau) &= 0, \\ \text{Cov}_x(\tau) &= \frac{2\Lambda_2}{\tau\gamma_1^2\gamma_2^3(\gamma_1 + \gamma_2)} \left((\alpha_m^2 - \alpha_s^2)(\bar{\beta}_2 + \gamma_2)\gamma_1^2 - (1 - \tau\gamma_1)\bar{\beta}_2^2\gamma_2(\gamma_1 + \gamma_2) \right) \\ &\quad + \frac{\Lambda_2}{\tau\gamma_1^2\gamma_2(\gamma_1 + \gamma_2)} \left(2\gamma_1\gamma_2 + 2\bar{\beta}_2\gamma_2 + (\alpha_m^2 - \alpha_s^2)^2 \right) e^{-\gamma_1\tau} \\ &\quad - \frac{\Lambda_2(\bar{\beta}_2 + \gamma_2)(\alpha_m^2 - \alpha_s^2)}{\tau\gamma_1^2\gamma_2^3(\gamma_1 + \gamma_2)} \left(\gamma_2^2 + 2\gamma_1(\gamma_1 + \gamma_2) + \tau\gamma_2^2(\gamma_1 + \gamma_2) \right) e^{-\gamma_2\tau}, \\ \text{Cov}_y(\tau) &= \frac{2\Lambda_1}{\tau\gamma_1^3\gamma_2^2(\gamma_1 + \gamma_2)} \left((\alpha_m^1 - \alpha_s^1)(\bar{\beta}_1 + \gamma_1)\gamma_2^2 - (1 - \tau\gamma_2)\bar{\beta}_1^2\gamma_1(\gamma_1 + \gamma_2) \right) \\ &\quad + \frac{\Lambda_1}{\tau\gamma_1\gamma_2^2(\gamma_1 + \gamma_2)} \left(2\gamma_1\gamma_2 + 2\bar{\beta}_1\gamma_1 + (\alpha_m^1 - \alpha_s^1)^2 \right) e^{-\gamma_2\tau} \\ &\quad - \frac{\Lambda_1(\bar{\beta}_1 + \gamma_1)(\alpha_m^1 - \alpha_s^1)}{\tau\gamma_1^3\gamma_2^2(\gamma_1 + \gamma_2)} \left(\gamma_1^2 + 2\gamma_2(\gamma_1 + \gamma_2) + \tau\gamma_1^2(\gamma_1 + \gamma_2) \right) e^{-\gamma_1\tau}. \end{aligned}$$

Remark 20 *It is of interest to expand the lead-lag relation given by Proposition 11 but it leads to equations far too large.*

Lastly, the expansion of the diffusive limit volatility is explicitly known.

Proposition 21 *The first order Taylor expansion (with respect to a and y) of the diffusive limit σ_{11}^2 , σ_{22}^2 and the correlation associated with the matrix of Proposition 14 is given by:*

$$\begin{aligned}\sigma_{11}^2 &= \frac{\nu_1^2}{4} \left(2\kappa_1^2 \Lambda_1 + \frac{2\kappa_1^2}{\theta_1} \Lambda_2 x \right), \\ \sigma_{22}^2 &= \frac{\nu_2^2}{4} \left(2\kappa_2^2 \Lambda_2 + \frac{2\kappa_2^2}{\theta_2} \Lambda_1 y \right), \\ \rho &= \frac{\sigma_{12}}{\sigma_{11}\sigma_{22}} = \frac{\kappa_1}{\kappa_2} \sqrt{\frac{\Lambda_1}{\Lambda_2}} \frac{y}{\gamma_2} + \frac{\kappa_2}{\kappa_1} \sqrt{\frac{\Lambda_2}{\Lambda_1}} \frac{x}{\gamma_1}.\end{aligned}$$

We note that an increase of x increases both σ_{11} and ρ and a similar conclusion applies to y .

3.5 Impact of stock up and down moves

The analytical results enable us to further develop the model properties. In fact, it is possible to explicitly analyze the impact of an up or down move of one asset on the other as well as on itself. This is a key quantity to understand the interaction between the assets. We illustrate the impact of an “up” move of the second asset on the first and second asset but similar results apply to a “down” move.

Proposition 22 *Suppose τ and δ are two positive real numbers, the impact on the first stock of an “up” move on the second stock returns computed over a time interval of length τ is:*

$$Imp(\tau, \delta) = \lim_{t \rightarrow +\infty} \mathbb{E} \left[S_{t+\tau+\delta}^1 - S_{t+\delta}^1 | dN_t^{2,u} = 1 \right] \quad (51)$$

$$= \frac{\nu_1}{2\bar{\lambda}_\infty^{2,u}} (M_{13} - M_{23}) \quad (52)$$

with $M = c_2(\tau)c_0(\delta)(\bar{\Lambda}_\infty + \alpha \text{diag}(\bar{\lambda}_\infty))$ and $\bar{\lambda}_\infty = \left(\bar{\lambda}_\infty^{1,u}, \bar{\lambda}_\infty^{1,d}, \bar{\lambda}_\infty^{2,u}, \bar{\lambda}_\infty^{2,d} \right)^\top$ is defined by Eq.(11).

It might be convenient to consider the stock evolution over an infinitesimal interval. From the previous proposition it is straightforward to deduce the next result.

Proposition 23 *Given the impact function (51) then the infinitesimal impact function is given by:*

$$Imp(\delta) = \lim_{\tau \rightarrow 0} \frac{Imp(\tau, \delta)}{\tau} \quad (53)$$

$$= \frac{\nu_1}{2\bar{\lambda}_\infty^{2,u}} (M_{13}(\delta) - M_{23}(\delta)) \quad (54)$$

with $M = c_0(\delta)(\bar{\Lambda}_\infty + \alpha \text{diag}(\bar{\lambda}_\infty))$.

It is often meaningful to consider the *cumulative* impact of a stock move which amount to integrate with respect to δ the above quantity. Simple computations give the next proposition.

Proposition 24 *Given the function $\text{Imp}(\delta)$ of Proposition 23 then the cumulative price impact of trades up to a given time t is:*

$$\begin{aligned} \text{Cimp}(t) &= \int_0^t \text{Imp}(\delta) d\delta \\ &= \frac{\nu_1}{2\bar{\lambda}_\infty^{2,u}} (M_{13}(t) - M_{23}(t)) \end{aligned} \quad (55)$$

with $M(t) = \int_0^t c_0(\delta) d\delta (\bar{\Lambda}_\infty + \alpha \text{diag}(\bar{\lambda}_\infty))$.

Lastly, performing a Taylor expansion with respect to the coupling parameters we obtain the next result.

Proposition 25 *Given the function $\text{Cimp}(t)$ of Proposition 24 then the Taylor expansion w.r.t x and y is given by:*

$$\text{Cimp}(t) = \text{Cimp}^0(t) + x \text{Cimp}_x(t) + y \text{Cimp}_y(t) \quad (56)$$

with

$$\begin{aligned} \text{Cimp}^0(t) &= (\tilde{M}^0(t))_{13} - (\tilde{M}^0(t))_{23}, \\ \text{Cimp}_x(t) &= (\tilde{M}_x(t))_{13} - (\tilde{M}_x(t))_{23}, \\ \text{Cimp}_y(t) &= (\tilde{M}_y(t))_{13} - (\tilde{M}_y(t))_{23} \end{aligned}$$

with the matrices $\tilde{M}^0(t)$, $\tilde{M}_x(t)$ and $\tilde{M}_y(t)$ given in the appendix.

It is possible to check that $\text{Cimp}^0(t) = 0$ and it is an intuitive result as $x = y = 0$ implies that the two stocks are not related, so an up (or down) jump of the second asset has no impact on the first one.

$\text{Cimp}_x(t)$ and $\text{Cimp}_y(t)$ can be explicitly computed but the expressions are rather lengthy.

Remark 26 *The expression for the infinitesimal price impact of an up move of the first asset on the second asset is given by $\frac{\nu_1}{2\bar{\lambda}_\infty^{1,u}} (M_{31}(\delta) - M_{41}(\delta))$ (and completes the Proposition 23). For the infinitesimal impact of an up move of the first asset on itself the expression is given by $\frac{\nu_1}{2\bar{\lambda}_\infty^{1,u}} (M_{11}(t) - M_{21}(t))$ and the zero order (in x and y) Taylor expansion for this expression allows us to recover the expression obtained in Da Fonseca and Zaatour (2015).*

4 Empirical Analysis

4.1 Data description and estimation methodology

We rely on tick-by-tick data from TRTH (Thomson Reuters Tick History)⁵. We deal with futures on indices such as Dax and Eurostoxx (respectively denoted FDX and STXE in the tables), as well as some other stocks : Renault, Peugeot, Société Générale and BNP Paribas (respectively RENA.PA, PEUP.PA, SOGN.PA and BNPP.PA). The data cover the period between 2010/01/01 to 2011/12/31. It consists of quote files recording quote changes (bid/ask prices and quantities) time stamped up to the millisecond, as well as trade files recording the transactions (prices and quantities) time stamped up to the millisecond. For every considered day, we take the front maturing futures for the indices, i.e the futures with nearest maturity, which is generally the most traded one. For every considered asset, we neglect the first and last 15 minutes in order to avoid the open and close auctions.

The estimation algorithm relies on the maximum likelihood method. From Proposition 7.2.III of Daley and Jones (2002), the log-likelihood of a point process $(N_t)_{t \geq 0}$ writes up to an additive constant:

$$\begin{aligned} L &= - \int_0^T \mathbf{1}^\top \lambda_t dt + \int_0^T \ln(\lambda_t)^\top dN_t \\ &= - \int_0^T \left(\lambda_\infty + \int_0^t e^{-\beta(t-s)} \alpha dN_s \right)^\top \mathbf{1} dt + \sum_{i=1}^n \sum_{j=1}^{N_T^i} \ln \left(\lambda_{t_j^i}^i \right), \end{aligned}$$

where t_j^i is the j -th jump of the i -th component, so that the log-likelihood of the multidimensional Hawkes process is the sum of the log-likelihoods generated by the observation of each coordinate process:

$$L = \sum_{m=1}^n L_m.$$

This takes a particularly simple form if we consider a diagonal structure for the β matrix, that is $\beta = \text{diag}(\bar{\beta}_1, \dots, \bar{\beta}_n)$, we obtain thanks to Ogata (1981):

$$L_m = -\lambda_\infty^m T - \sum_{j=1}^{N_T^m} \sum_{i=1}^n \frac{\alpha_{mi}}{\bar{\beta}_m} \left(1 - e^{\bar{\beta}_i(T-t_j^m)} \right) + \sum_{j=1}^{N_T^m} \ln \left[\lambda_\infty^m + \sum_{i=1}^n \alpha_{mi} R^{mi}(j) \right],$$

⁵Part of the data are provided by SIRCA <http://www.sirca.org.au/>.

where:

$$\begin{aligned}
R^{mi}(1) &= 0, \\
R^{mm}(j) &= e^{-\bar{\beta}_m(t_j^m - t_{j-1}^m)}(1 + R^{mm}(j-1)), \\
R^{mi}(j) &= e^{-\bar{\beta}_m(t_j^m - t_{j-1}^m)}R^{mi}(j-1) + \sum_{k: t_{j-1}^m \leq t_k^i < t_j^m} e^{-\bar{\beta}_m(t_j^m - t_k^i)} \text{ for } i \neq m.
\end{aligned}$$

These recursive equations enable a very efficient calculation of the likelihood function⁶.

We estimate the model as described in Eq.(28). The calibration strategy consists in beginning by calibrating the two Hawkes processes characterizing each stock alone. This gives rise to two calibration problems with four parameters each, namely $\lambda_\infty^i, \alpha_s^i, \alpha_s^i, \bar{\beta}_s^i$ where first guesses for $\lambda_\infty^i, \alpha_s^i, \alpha_s^i$ are taken to be a fraction of the Poisson lambda of the observed process (we take tenth). There the Poisson lambda is the intensity of a Poisson process with the same mean as the data, and $\bar{\beta}^i$ is taken to ensure the stability condition. Once this calibration is solved, we turn to the entire problem, which has 10 parameters. First guesses for the β^i are taken to be the formerly found ones in the preceding calibration. First guesses for the other parameters are half of the first parameters calibrated in the preceding procedure, to let some room for the new exciting parameters x and y . First guesses for x and y are taken to be equal to the mean of all α 's. For MLE maximization, we rely on the Nelder-Mead algorithm as implemented in the open source library NL-opt⁷. Notice that at every optimization step, we check the stability condition specified by Eq.(32) and Eq.(33) are satisfied.

4.2 Estimation results

Results are gathered in Table I. The table gives means, median and standard deviations for daily calibrated parameters.

[Insert Table I here]

In order to read the table, and in accordance with our previous notations, notice that for every pair (A,B), the value of x carries the influence of B on A, and the value of y carries the influence of A on

⁶Note that an even more efficient (in terms of computational speed) estimation algorithm can be developed using the moments and the autocorrelation function, see Da Fonseca and Zaatour (2014) for an example, but it is not the purpose of this paper to focus on calibration speed.

⁷<http://ab-initio.mit.edu/wiki/index.php/NLopt>

B.

We are naturally primarily interested in the coupling parameters x and y so a closer look is achieved by plotting the time series for these pairs. In Figure 3, one can see that for the pair (SOGN.PA,BNPP.PA), x and y take heterogeneous values. There are some periods where one clearly dominates the other, and other periods where these values are not so far apart. The leader and lagger roles are shared by the two banks over the sample.

For the pair formed by the (STXE, BNPP.PA) the roles are clearly identified, as futures on the index clearly leads the stock.

[Insert Figure 3 here]

In Figure 4, one can see that for the pair of stocks (RENA.PA, PEUP.PA) results are different than for the banks. Indeed, x clearly dominates y which means that Peugeot influences Renault. This can be explained by two facts: first, Peugeot stock is cheaper than Renault (average price for the considered period is 24 Euro for Peugeot and 35 Euro for Renault) so that stakes on the automotive industry will be taken preferably on Peugeot than Renault as it will ensure a better leverage; secondly, the French state being one of the principal Renault stock holder, it suggests that automotive industry speculators are likely to focus on Peugeot in the first place.

Finally, the Eurostoxx naturally leads the DAX German index and the former is based on the largest European companies while the latter only depends on German companies.

[Insert Figure 4 here]

These lead-lag relationships can also be expressed in terms of time. Indeed, we have seen in Figure 2 that the correlation induced by a Hawkes framework, when x and y are different, reaches its maximum value when returns are calculated during two (overlapping) periods with a certain lag. This time lag can be used to characterize the lead-lag relationship. Indeed, for a given pair (A,B) if $x > y$ then B influences A, the maximum correlation is achieved with a positive lag and it will be negative otherwise. Once our models are calibrated, we can calculate this optimal lag daily, which gives the Table II.

[Insert Table II here]

Lastly, we report in Figure 5 the infinitesimal impact functions of an up move of the second asset on the first asset and an up move of the first asset on the second asset for the pair (STXE, SOGN.PA). These functions are given by Proposition 23 and Remark 26.

[Insert Figure 5 here]

We observe that an up move of the STXE has an immediate impact on SOGN.PA whereas an up move of SOGN.PA will have a maximum impact of STXE with a delay. The net effect is that STXE leads SOGN.PA. Note that we had to scale the curves by their values at 0.

5 Conclusion

In this paper we develop a multi-asset model using Hawkes process in the spirit of Bacry et al. (2013a). Within that framework we compute various statistical properties such as the signature plot, the covariance and the lagged covariance between the stocks. It allows us to precisely analyze the lead-lag relationship between the stocks, this is an important quantity that was, and still is, well studied within other frameworks (e.g. De Jong and Nijman (1997)). We perform some Taylor expansions for these quantities in order to gain a better understanding of the impact of the parameters on these key quantities. We also compute the diffusive limit associated with the model, thereby connecting the parameters driving the high-frequency dynamic with the low frequency (i.e. daily) evolution of the stocks. We find that it is not possible to capture this lead-lag relationship at low frequency, a result that confirms previous works (e.g. Huth and Abergel (2014)).

We estimate the model using a two-year sample of high-frequency data for two index futures and four major stocks quoted on the Eurex market. We find that the Eurostoxx leads all the stocks which is a somewhat expected result as it is the largest European index. For the same reasons we find that the Eurostoxx also leads the DAX. For the two stocks in the banking sector when averaged over the sample none of them clearly leads the other. However, when the lead-lag relationship is analyzed at a daily frequency we find some periods during which one stock clearly leads the other. For the two stocks of the automotive industry one of the stock systematically leads the other and it is consistent with the shareholder structure of these companies (one of them is partially state owned). Overall, the results are consistent with financial intuition.

Our work suggests several extensions. The same framework can be used to analyze the interactions between orders of different types (i.e. cancellation, amend, market and limit orders) for a given stock. It will provide us with a better understanding of the micro foundation of the stock price dynamic and the diffusive limit results would allow us to quantify the contribution of these orders to the daily volatility. It would complete the existing works on that subject (e.g. Chiarella et al. (2009) and Eisler et al. (2012)). The same framework could be used in conjunction with a modelling of the volume to define the stock price dynamic. It would require to extend the analytical results and specify how the volume is related to the jumps of the Hawkes process (supposed to represent an order). The objective would be to keep the results tractable so that the diffusive limit could be computed. Along these lines let us quote the works of Cont and De Larrard (2013) and Cont and De Larrard (2012). Let us also mention the interesting contribution of Bacry and Muzy (2014a) where price and trade are simultaneously modeled for a single stock. Lastly, putting these results into an optimal order execution perspective is certainly of interest and a challenging task, along this line see Alfonsi and Blanc (2014).

References

- F. Abergel and A. Jedidi. A Mathematical Approach to Order Book Modeling. *International Journal of Theoretical and Applied Finance*, 16(5):1350025, 2013. doi: 10.1142/S0219024913500258.
- Y. Aït-Sahalia, J. Cacho-Diaz, and R. J.A. Laeven. Modeling financial contagion using mutually exciting jump processes. Technical report.
- A. Alfonsi and P. Blanc. Dynamic optimal execution in a mixed-market-impact Hawkes price model. *Working Paper arXiv:1404.0648*, 2014.
- E. Bacry and J.-F. Muzy. Hawkes model for price and trades high-frequency dynamics. *Quantitative Finance*, 14(7), 2014a. doi: 10.1080/14697688.2014.897000.
- E. Bacry and J.-F. Muzy. Second order statistics characterization of Hawkes processes and non-parametric estimation. Available at <http://www.cmap.polytechnique.fr/~bacry/ftpPapers.html>, 2014b.
- E. Bacry, K. Dayri, and J.-F. Muzy. Non-parametric kernel estimation for symmetric Hawkes processes. Application to high frequency financial data. *The European Physical Journal B - Condensed Matter and Complex Systems*, 85(5): 1–12, May 2012. doi: 10.1140/epjb/e2012-21005-8.
- E. Bacry, S. Delattre, M. Hoffmann, and J.-F. Muzy. Modelling microstructure noise with mutually exciting point processes. *Quantitative Finance*, 13(1):65–77, Jan. 2013a. doi: 10.1080/14697688.2011.647054.
- E. Bacry, S. Delattre, M. Hoffmann, and J.-F. Muzy. Scaling limits for hawkes processes and application to financial statistics. *Stochastic Processes and Applications*, 123(12):2475–2499, 2013b. doi: 10.1016/j.spa.2013.04.007.
- C. G. Bowsher. Modelling security market events in continuous time: Intensity based, multivariate point process models. *Journal of Econometrics*, 141:876–912, 2007. doi: 10.1016/j.jeconom.2006.11.007.
- P. Brémaud and L. Massoulié. Imbedded construction of stationary sequences and point processes with a random memory. *Queueing Systems*, 17:213–234, 1994. doi: 10.1007/BF01158695.
- K. Chan. A further analysis of the lead–lag relationship between the cash market and stock index futures market. *The Review of Financial Studies*, 5(1):123–152, 1992. ISSN 08939454.
- C. Chiarella, G. Iori, and J. Perelló. The impact of heterogeneous trading rules on the limit order book and order flows. *Journal of Economic Dynamics and Control*, 33(3):525–537, 2009. doi: 10.1016/j.jedc.2008.08.001.
- R. Cont and A. De Larrard. Order Book Dynamics in Liquid Markets: Limit Theorems and Diffusion Approximations. *arXiv:1202.6412*, Feb. 2012.
- R. Cont and A. De Larrard. Price dynamics in a Markovian limit order book market. *SIAM Journal for Financial Mathematics*, 4(1):1–25, Jan. 2013. doi: 10.1137/110856605.
- J. Da Fonseca and R. Zaatour. Hawkes process: Fast calibration, application to trade clustering and diffusive limit. *Journal of Futures Markets*, 34(6):548–579, June 2014. doi: 10.1002/fut.21644.
- J. Da Fonseca and R. Zaatour. Clustering and mean reversion in a Hawkes microstructure model. *Journal of Futures Markets*, 35(9):813–838, September 2015. doi: 10.1002/fut.21676.
- D. J. Daley and D. V. Jones. *An introduction to the theory of point processes, Vol 1, Elementary theory and methods*. Springer, Berlin Heidelberg New York, 2nd edition, 2002.
- D. J. Daley and D. V. Jones. *An introduction to the theory of point processes, Vol 2, General theory and structure*. Springer, Berlin Heidelberg New York, 2nd edition, 2008.
- F. De Jong and M. W. M. Donders. Intraday lead-lag relationships between the futures-, options and stock market. *European Finance Review*, 1(3):337–359, 1998. doi: 10.1023/A:1009765322522.
- F. De Jong and T. Nijman. High frequency analysis of Lead-Lag relationships between financial markets. *Journal of Empirical Finance*, 4:259–277, 1997. doi: 10.1016/S0927-5398(97)00009-1.
- Z. Eisler, J.-P. Bouchaud, and J. Kockelkoren. The price impact of order book events: market orders, limit orders and cancellations. *Quantitative Finance*, 12(9):1395–1419, 2012. doi: 10.1080/14697688.2010.528444.
- E. Errais, K. Giesecke, and L. R. Goldberg. Affine point processes and portfolio credit risk. *SIAM Journal on Financial Mathematics*, 1(1):642–665, 2010. doi: 10.1137/090771272.

- A. Frino, T. Walter, and A. West. The leadlag relationship between equities and stock index futures markets around information releases. *Journal of Futures Markets*, 20(5):467–487, 2000. doi: 10.1002/(SICI)1096-9934(200005)20:5<467::AID-FUT4>3.0.CO;2-L.
- A. G. Hawkes. Spectra of some self-exciting and mutually exciting point processes. *Biometrika*, 58(1):83–90, 1971. doi: 10.2307/2334319.
- A. F. Herbst, J. P. McCormack, and E. N. West. Investigation of a lead-lag relationship between spot stock indices and their futures contracts. *Journal of Futures Markets*, 7(4):373–381, 1987. doi: 10.1002/fut.3990070403.
- P. Hewlett. Clustering of order arrivals, price impact and trade path optimisation. 2006.
- M. Hoffmann, M. Rosenbaum, and N. Yoshida. Estimation of the lead-lag parameter from non-synchronous data. *Bernoulli*, 19(2):426–461, 2013. doi: doi:10.3150/11-BEJ407.
- N. Huth and F. Abergel. High Frequency Lead/lag Relationships Empirical facts. *Journal of Empirical Finance*, 26: 41–58, March 2014. doi: 10.1016/j.jempfin.2014.01.003.
- A. Jedidi and F. Abergel. On the Stability and Price Scaling Limit of a Hawkes Process-Based Order Book Model. *Working paper available at <http://hal.archives-ouvertes.fr/hal-00821607>*, 2013.
- A. Kirilenko, R. B. Sowers, and X. Meng. A multiscale model of high-frequency trading. *Algorithmic Finance*, 2(1): 59–98, Feb. 2013. doi: 10.3233/AF-13017.
- J. Large. Measuring the resiliency of an electronic limit order book. *Journal of Financial Markets*, 10(1):1–25, February 2007. doi: 10.1016/j.finmar.2006.09.001.
- Y. Ogata. On Lewis simulation method for point processes. *IEEE Transactions on Information Theory*, 27(1):23–31, 1981. doi: 10.1109/TIT.1981.1056305.
- P. Protter. *Stochastic Integration and Differential Equations*. Stochastic Modelling and Applied Probability. Springer-Verlag, Berlin Heidelberg New York, 2nd edition, 2004.
- D. Revuz and M. Yor. *Continuous martingales and Brownian motion*. Springer, Berlin Heidelberg New York, 3rd edition, 1999.

Tables

Table I: Calibration Results

Pair	Measure	$\lambda_{1,\infty}$	α_s^1	α_m^1	β^1	$\lambda_{2,\infty}$	α_s^2	α_m^2	β^2	x	y
STXE,SOGN.PA	Mean	0.0111	0.0049	0.0601	0.1215	0.0556	0.1797	0.0928	0.6028	0.0059	0.2488
	Median	0.0075	0.0011	0.0528	0.0899	0.0352	0.0329	0.0169	0.3465	0.0000	0.1891
	Std. dev.	0.0133	0.0085	0.0358	0.1109	0.0717	0.2601	0.1522	0.6379	0.0271	0.1920
STXE,BNPP.PA	Mean	0.0114	0.0039	0.0553	0.1028	0.0580	0.1041	0.0712	0.4260	0.0057	0.2156
	Median	0.0079	7e-04	0.0487	0.0772	0.0363	1e-04	0.0072	0.2100	0.0000	0.1650
	Std. dev.	0.0119	0.0074	0.0341	0.0943	0.0622	0.2245	0.1587	0.5926	0.0265	0.2038
STXE,RENA.PA	Mean	0.0081	0.0039	0.0636	0.0960	0.0324	0.1169	0.0833	0.4630	0.0018	0.2028
	Median	0.0055	7e-04	0.0572	0.0793	0.0249	0.0358	0.0208	0.2537	0.0000	0.1683
	Std. dev.	0.0097	0.0075	0.0343	0.0711	0.0313	0.1680	0.1306	0.5037	0.0150	0.1446
STXE,PEUP.PA	Mean	0.0051	0.0029	0.0615	0.0816	0.0130	0.0383	0.0535	0.2178	0.0058	0.1223
	Median	0.0035	9e-04	0.0559	0.0719	0.0110	0.0080	0.0380	0.1531	0.0000	0.1117
	Std. dev.	0.0058	0.0049	0.0292	0.0528	0.0103	0.0592	0.0619	0.1936	0.0221	0.0670
STXE,FDX	Mean	0.0086	0.0032	0.0604	0.0860	0.0510	2e-04	0.0066	0.0710	1e-04	0.0706
	Median	0.0072	0.0016	0.0517	0.0714	0.0496	0.0000	0.0000	0.0619	0.0000	0.0619
	Std. dev.	0.0082	0.0045	0.0373	0.0678	0.0294	8e-04	0.0131	0.0357	4e-04	0.0354
SOGN.PA,BNPP.PA	Mean	0.0263	0.0845	0.2012	0.5604	0.0382	0.1103	0.1907	0.6488	0.2271	0.2575
	Median	0.0184	0.0031	0.1515	0.3416	0.0283	0.0172	0.1440	0.4296	0.1610	0.1845
	Std. dev.	0.0276	0.1727	0.2213	0.6180	0.0343	0.2280	0.2302	0.7615	0.2844	0.2846
RENA.PA,PEUP.PA	Mean	0.0185	0.0830	0.0460	0.3353	0.0150	0.0734	0.1147	0.3992	0.2173	0.0638
	Median	0.0132	0.0014	1e-04	0.1643	0.0113	0.0511	0.0943	0.2649	0.1840	0.0378
	Std. dev.	0.0205	0.1348	0.0855	0.4060	0.0185	0.0855	0.0823	0.4514	0.1547	0.0847

Note. Mean, median and standard deviation of calibration results for the different pairs.

Table II: Lead Times

Pair	Mean	Median	Std. dev.
STXE,SOGN.PA	-2.39	-2	3.06
STXE,BNPP.PA	-3.38	-3	3.53
STXE,RENA.PA	-3.04	-3	2.90
STXE,PEUP.PA	-3.89	-3	4.05
STXE,FDX	-9.56	-9	4.55
SOGN.PA,BNPP.PA	0.14	0	2.12
RENA.PA,PEUP.PA	4.23	3	4.66

Note. Mean, median and standard deviation of lead times. A negative value t indicates that maximum correlation between the components of the pair is attained if we measure the increments of the second pair component t seconds after those of the first component.

Figures

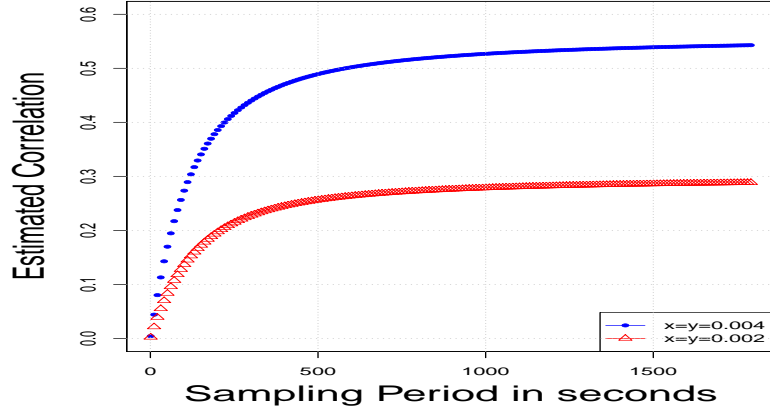


Figure 1: Illustration of the Epps effect reconstruction. We considered perfectly symmetric stocks, with $\alpha_s = \alpha_m = 0.004$ and considered two values for the coupling coefficients x and y . Notice that when these latter are halved, the asymptotic correlation is always roughly halved. Notice also that the time taken to reach the asymptotic correlation does not depend on the coupling coefficients.

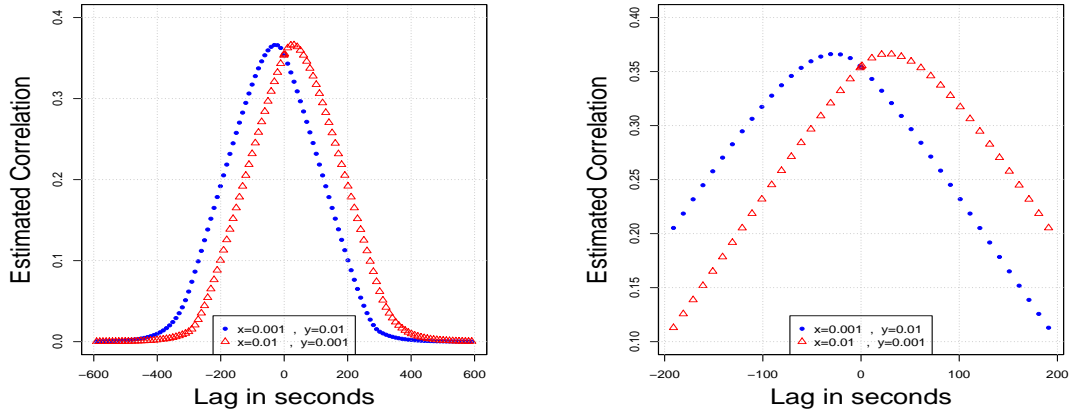


Figure 2: Illustration of the asymmetry of the correlation induced by a Hawkes process. We considered perfectly symmetric stocks, with $\alpha_s^1 = \alpha_s^2 = \alpha_m^1 = \alpha_m^2 = 0.004$ and considered two values for the coupling coefficients x and y . The figures report $\delta \rightarrow \mathcal{C}(\tau, \delta)$ for $\delta \in \mathbb{R}$ with the function \mathcal{C} defined in Proposition 11 for two pairs of values for (x, y) ; the first one is $(0.001, 0.01)$ and gives the blue-bullet curve, the second one is $(0.01, 0.001)$ and gives the red-triangle curve. In the right figure, a zoom around zero lag is performed to help to visualize the fact that maximum correlation is achieved for a certain lag.

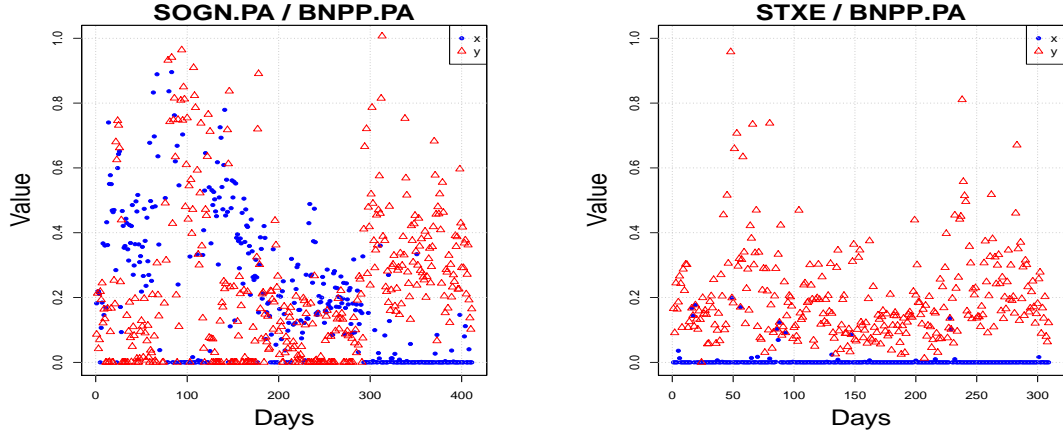


Figure 3: We plot time series of the daily calibrated parameters x (blue-bullet points) and y (red-triangle points) for the pairs (SOGN.PA, BNPP.PA) on the left and (STXE,BNPP.PA) on the right, illustrating the evolution of the respective lead lag relationships in time. Notice that the index systematically leads the stock as is clear in the right figure. The relationship between Société Générale and BNP Paribas is more mitigated, even that beginning April 2011, the two stocks began a bearish period, where Société Générale is clearly the leader.

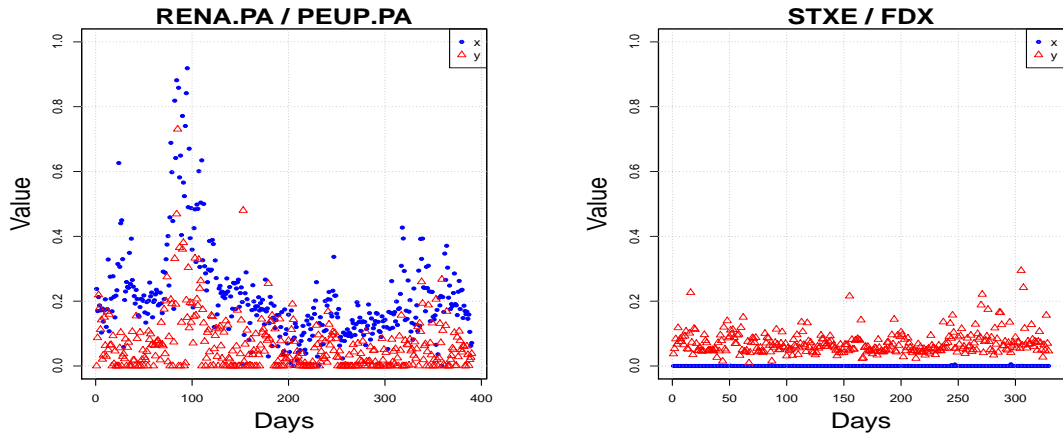


Figure 4: We plot time series of the daily calibrated parameters x (blue-bullet points) and y (red-triangle points) for the pairs (RENA.PA, PEUP.PA) on the left and (STXE,FDX) on the right, illustrating the evolution of the respective lead lag relationships in time. The European index systematically leads the German index, while Peugeot systematically leads Renault, even if the feedback effect here is more pronounced than in the case of the indices.

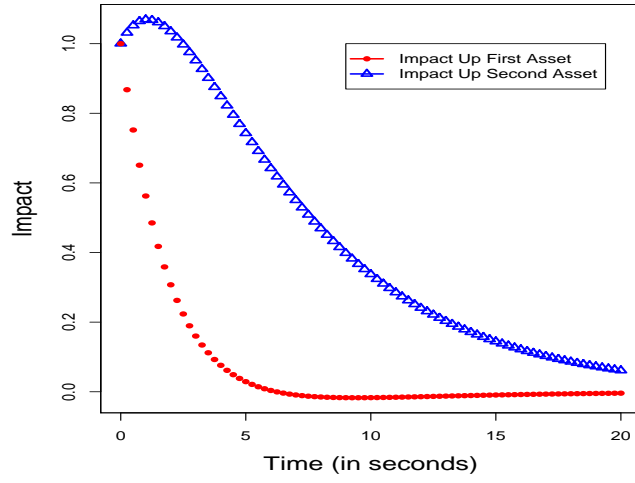


Figure 5: We plot the infinitesimal impact functions for an up move of the second asset on the first asset (i.e. Proposition 23) and the first asset on the second (i.e. Remark 26). We use estimates of Table I and report values for the pair (STXE,SOGN.PA). The functions are normalized by their values at 0 to fit correctly in a single figure. The impact of an up move of the first asset (STXE) on the second asset (SOGN.PA) is immediate whereas the impact of an up move of the second asset (SOGN.PA) on the first one (i.e. STXE) is delayed, and the net effect is that STXE leads SOGN.PA. We took $\nu_1 = \nu_2 = 2$ to cancel the influence of these parameters.

Appendix

Proof. of Lemma 1

Taking into account the fact that $dN_t - \lambda_t dt$ is a martingale we deduce Eq.(7). We rewrite the dynamic Eq.(1) as

$$d\lambda_t = \beta(\lambda_\infty - \lambda_t)dt + \alpha(dN_t - \lambda_t dt) + \alpha\lambda_t dt$$

and using again the martingale property of $dN_t - \lambda_t dt$ we deduce Eq.(6) after taking the expectation. ■

Proof. of Lemma 3

This result appears for example in Da Fonseca and Zaatour (2015). Let us reproduce here the proof with a small variation in the argumentation that makes a more explicit reference to Chapter II section 6 of Protter (2004). Following this reference we have:

$$d(N_t N_t^\top) = dN_t N_t^\top + N_t dN_t^\top + d[N., N.]_t$$

and as $dN_t N_t^\top = (dN_t - \lambda_t dt)N_t^\top + \lambda_t N_t^\top dt$, $d[N., N.]_t = \text{diag}(dN_t)$ (the diagonal form is due to the fact that no simultaneous jumps can occur) combined with the martingale property of $dN_t - \lambda_t dt$ we deduce Eq.(14) after taking the expectation.

To obtain Eq.(15) we proceed as follows:

$$d(\lambda_t N_t^\top) = d\lambda_t N_t^\top + \lambda_t dN_t^\top + d[\lambda., N.]_t.$$

As we have:

$$\begin{aligned} d\lambda_t N_t^\top &= (\beta(\lambda_\infty - \lambda_t)dt + \alpha dN_t)N_t^\top \\ &= \beta(\lambda_\infty - \lambda_t)N_t^\top dt + \alpha(dN_t - \lambda_t dt)N_t^\top + \alpha\lambda_t N_t^\top dt \end{aligned}$$

and $\lambda_t dN_t^\top = \lambda_t(dN_t^\top - \lambda_t^\top dt) + \lambda_t \lambda_t^\top dt$ and $d[\lambda., N.]_t = \alpha \text{diag}(dN_t)$ we obtain the result.

To obtain Eq.(16) we proceed along the same lines using the fact that $d[\lambda., \lambda.]_t = \alpha \text{diag}(dN_t)\alpha^\top$. Direct integration gives the equations Eq.(9) and Eq.(10) after using the fact that $dN_t - \lambda_t dt$ is a martingale. ■

Proof. of Proposition 14

The result is obtained by direct computation but we recommend the use of a symbolic calculator. The code leading to the results is available upon request. ■

Proof. of Proposition 18

To perform the expansion we need to differentiate the function Eq.(18). Let us define $\alpha_x = \frac{d\alpha}{dx}$, $\alpha_y = \frac{d\alpha}{dy}$, $\alpha^0 = \alpha_{x=0, y=0}$. Starting from $I = \alpha^{-1}\alpha$ and taking into account the fact that β does not depend on x and y we deduce:

$$\begin{aligned} (\alpha^{-1})_x &= -\alpha^{-1}\alpha_x\alpha^{-1} \\ ((\alpha - \beta)^{-1})_x &= -(\alpha - \beta)^{-1}\alpha_x(\alpha - \beta)^{-1} \end{aligned}$$

(these equations will be evaluated for $\alpha = \alpha^0$) and similarly:

$$\begin{aligned} (\alpha^{-2})_x &= -\alpha^{-2}(\alpha_x\alpha + \alpha\alpha_x)(\alpha^2)^{-1} \\ &= -\alpha^{-2}\alpha_x\alpha^{-1} - \alpha^{-1}\alpha_x\alpha^{-2}. \end{aligned}$$

For example, from the previous equation we deduce that:

$$((\alpha - \beta)^{-2})_x = -(\alpha - \beta)^{-2}\alpha_x(\alpha - \beta)^{-1} - (\alpha - \beta)^{-1}\alpha_x(\alpha - \beta)^{-2}.$$

From the equation $\bar{\lambda}_\infty = -(\alpha - \beta)^{-1}\beta\lambda_\infty$ we define:

$$\begin{aligned} \bar{\lambda}_\infty^0 &= -(\alpha^0 - \beta)^{-1}\beta\lambda_\infty \\ \bar{\lambda}_{x,\infty}^0 &= \left(\frac{d\bar{\lambda}_\infty}{dx}\right)_{x=0} = ((\alpha^0 - \beta)^{-1}\alpha_x(\alpha^0 - \beta)^{-1})\beta\lambda_\infty \end{aligned}$$

with similar equation for $\bar{\lambda}_{y,\infty}^0$. We expand $\bar{\lambda}_\infty$ solution of:

$$(\alpha - \beta)\bar{\lambda}_\infty + \bar{\lambda}_\infty(\alpha - \beta)^\top + \alpha \text{diag}(\bar{\lambda}_\infty)\alpha^\top = 0$$

in the form $\bar{\lambda}_\infty = \bar{\lambda}_\infty^0 + x\bar{\lambda}_{x,\infty}^0 + y\bar{\lambda}_{y,\infty}^0$ with:

$$(\alpha^0 - \beta)\bar{\lambda}_\infty^0 + \bar{\lambda}_\infty^0(\alpha^0 - \beta)^\top + \alpha^0 \text{diag}(\bar{\lambda}_\infty^0)(\alpha^0)^\top = 0$$

and

$$\begin{aligned} (\alpha^0 - \beta)\bar{\lambda}_{x,\infty}^0 + \bar{\lambda}_{x,\infty}^0(\alpha^0 - \beta)^\top &= -\alpha_x \bar{\lambda}_\infty^0 - \bar{\lambda}_\infty^0 \alpha_x^\top - \alpha_x \text{diag}(\bar{\lambda}_\infty^0)(\alpha^0)^\top \\ &\quad - \alpha^0 \text{diag}(\bar{\lambda}_{x,\infty}^0)(\alpha^0)^\top - \alpha^0 \text{diag}(\bar{\lambda}_\infty^0)\alpha_x^\top \end{aligned}$$

with a similar equation for $\bar{\lambda}_{y,\infty}^0$.

We need to differentiate $\text{Cov}(\tau)$ given by Eq.(18), it leads to differentiate $c_5(\tau)$ of Eq.(19). We denote $c_5^0(\tau)$ the function evaluated for $x = y = 0$ and the derivative is just:

$$\begin{aligned} \partial_x c_5(\tau)|_{x=y=0} &= \partial_x c_5^0(\tau) \\ &= (\alpha^0 - \beta)^{-1} \alpha_x (\alpha^0 - \beta)^{-1} \tau + \tau (\alpha^0 - \beta)^{-2} \alpha_x e^{(\alpha^0 - \beta)\tau} \\ &\quad - \left((\alpha^0 - \beta)^{-2} \alpha_x (\alpha^0 - \beta)^{-1} + (\alpha^0 - \beta)^{-1} \alpha_x (\alpha^0 - \beta)^{-2} \right) (e^{(\alpha^0 - \beta)\tau} - I). \end{aligned}$$

Lastly, the expansion of J_1 is:

$$\begin{aligned} J_1 &= J_1^0 + xJ_{1,x}^0, \\ J_1^0 &= c_5^0(\tau)(\bar{\lambda}_\infty^0 + \alpha \text{diag}(\bar{\lambda}_\infty^0)), \\ J_{1,x}^0 &= \partial_x c_5^0(\tau)(\bar{\lambda}_\infty^0 + \alpha^0 \text{diag}(\bar{\lambda}_\infty^0)) + c_5^0(\tau)(\bar{\lambda}_{x,\infty}^0 + \alpha_x \text{diag}(\bar{\lambda}_\infty^0) + \alpha^0 \text{diag}(\bar{\lambda}_{x,\infty}^0)). \end{aligned}$$

Therefore, we have the expansion for $\text{Cov}(\tau)$ given by:

$$\begin{aligned} \text{Cov}(\tau) &= J_1^0 + (J_1^0)^\top + \tau \text{diag}(\bar{\lambda}_\infty^0) \\ &\quad + x \left(J_{1,x}^0 + (J_{1,x}^0)^\top + \tau \text{diag}(\bar{\lambda}_{x,\infty}^0) \right) + y \left(J_{1,y}^0 + (J_{1,y}^0)^\top + \tau \text{diag}(\bar{\lambda}_{y,\infty}^0) \right) \end{aligned}$$

from which we can deduce the expansion of the signature plot. It still requires tedious computation and we recommend the use of a symbolic calculator. The code leading to the results is available upon request. ■

Proof. of Proposition 19

The result is obtained by direct computation but we recommend the use of a symbolic calculator. The code leading to the results is available upon request. ■

Proof. of Proposition 21

The result is obtained by direct computation but we recommend the use of a symbolic calculator. The code leading to the results is available upon request. ■

Proof. of Proposition 22

Given τ_0 , τ and δ the following quantity needs to be computed:

$$\begin{aligned} \mathbb{E}[(S_{t+\tau+\delta}^1 - S_{t+\delta}^1)(N_{t+\tau_0}^{2,u} - N_t^{2,u})] &= \frac{\nu_1}{2} \mathbb{E}[(N_{t+\tau+\delta}^{1,u} - N_{t+\delta}^{1,u})(N_{t+\tau_0}^{2,u} - N_t^{2,u})] \\ &\quad - \frac{\nu_1}{2} \mathbb{E}[(N_{t+\tau+\delta}^{1,d} - N_{t+\delta}^{1,d})(N_{t+\tau_0}^{2,u} - N_t^{2,u})]. \end{aligned} \tag{57}$$

As we have:

$$\begin{aligned} I_1 &= \mathbb{E}[(N_{t+\tau+\delta}^{1,u} - N_{t+\delta}^{1,u})(N_{t+\tau_0}^{2,u} - N_t^{2,u})] \\ &= \sum_{i=0}^{\infty} \mathbb{E}[N_{t+\tau+\delta}^{1,u} - N_{t+\delta}^{1,u} | N_{t+\tau_0}^{2,u} - N_t^{2,u} = i] \times \mathbb{P}[N_{t+\tau_0}^{2,u} - N_t^{2,u} = i] \times i. \end{aligned}$$

As we have:

$$\begin{aligned}\mathbb{P}[N_{t+\tau_0}^{2,u} - N_t^{2,u} = 1 | \mathcal{F}_t] &= \lambda_t^{2,u} \tau_0 + o(\tau_0) \\ \mathbb{P}[N_{t+\tau_0}^{2,u} - N_t^{2,u} > 1 | \mathcal{F}_t] &= o(\tau_0) \\ \mathbb{P}[N_{t+\tau_0}^{2,u} - N_t^{2,u} = 0 | \mathcal{F}_t] &= 1 - \lambda_t^{2,u} \tau_0 + o(\tau_0),\end{aligned}$$

then taking the limit $\tau_0 \rightarrow 0$ and for t large we deduce that:

$$\lim_{\tau_0 \rightarrow 0} \frac{I_1}{\tau_0} \sim \mathbb{E}[N_{t+\tau+\delta}^{1,u} - N_{t+\delta}^{1,u} | dN_t^{2,u} = 1] \bar{\lambda}_\infty^{2,u}.$$

Moreover, as we have:

$$\mathbb{E}[(N_{t+\tau+\delta}^{1,u} - N_{t+\delta}^{1,u})(N_{t+\tau_0}^{2,u} - N_t^{2,u})] = (\text{Cov}_1(\tau_0, \tau, \delta))_{13},$$

we obtain:

$$\mathbb{E}[N_{t+\tau+\delta}^{1,u} - N_{t+\delta}^{1,u} | dN_t^{2,u} = 1] = \frac{1}{\bar{\lambda}_\infty^{2,u}} (c_2(\tau) c_0(\delta) (\bar{\Lambda}_\infty + \alpha \text{diag}(\bar{\lambda}_\infty)))_{13}.$$

Similar computations can be carried out for Eq.(57) and the announced result is obtained.

■

Proof. of Proposition 25

We need to perform a Taylor expansion of $M(t) = \int_0^t c_0(\delta) d\delta (\bar{\Lambda}_\infty + \alpha \text{diag}(\bar{\lambda}_\infty))$. Note that the integral is in fact $c_2(t)$ of Lemma 1. We denote the expansions as

$$\begin{aligned}c_2(t) &= c_2^0(t) + x \partial_x c_2^0(t) + y \partial_y c_2^0(t) \\ \bar{\lambda}_\infty &= \bar{\lambda}_\infty^0 + x \bar{\lambda}_{x,\infty}^0 + y \bar{\lambda}_{y,\infty}^0 \\ \bar{\Lambda}_\infty &= \bar{\Lambda}_\infty^0 + x \bar{\Lambda}_{x,\infty}^0 + y \bar{\Lambda}_{y,\infty}^0 \\ \bar{\lambda}_\infty^{2,u} &= \bar{\lambda}_\infty^{0,2,u} + x \bar{\lambda}_{x,\infty}^{0,2,u} + y \bar{\lambda}_{y,\infty}^{0,2,u}.\end{aligned}$$

Performing a Taylor expansion of $\frac{1}{\bar{\lambda}_\infty^{2,u}} M(t)$ leads to

$$\begin{aligned}\frac{1}{\bar{\lambda}_\infty^{2,u}} M(t) &= \tilde{M}^0(t) + x \tilde{M}_x(t) + y \tilde{M}_y(t) \\ \tilde{M}^0(t) &= \frac{1}{\bar{\lambda}_\infty^{0,2,u}} c_2^0(t) (\bar{\Lambda}_\infty^0 + \alpha^0 \text{diag}(\bar{\lambda}_\infty^0)) \\ \tilde{M}_x(t) &= -\frac{\bar{\lambda}_{x,\infty}^{0,2,u}}{(\bar{\lambda}_\infty^{0,2,u})^2} c_2^0(t) (\bar{\Lambda}_\infty^0 + \alpha^0 \text{diag}(\bar{\lambda}_\infty^0)) + \frac{\partial_x c_2^0(t)}{\bar{\lambda}_\infty^{0,2,u}} (\bar{\Lambda}_\infty^0 + \alpha^0 \text{diag}(\bar{\lambda}_\infty^0)) \\ &\quad + \frac{c_2^0(t)}{\bar{\lambda}_\infty^{0,2,u}} (\bar{\Lambda}_{x,\infty}^0 + \alpha^0 \text{diag}(\bar{\lambda}_{x,\infty}^0) + \alpha_x \text{diag}(\bar{\lambda}_\infty^0))\end{aligned}$$

and similar expression for $M_y(t)$. The results are obtained by selecting the matrix elements (1,3) and subtracting the elements (2,3) and multiplying by $\frac{\nu_1}{2}$.

Note that

$$\partial_x c_2(t) = ((\alpha - \beta)^{-1})_x (e^{(\alpha - \beta)t} - I) + (\alpha - \beta)^{-1} \alpha_x e^{(\alpha - \beta)t} \quad (58)$$

this expression will be evaluated at $x = y = 0$, it leads to

$$\partial_x c_2^0(t) = ((\alpha^0 - \beta)^{-1})_x (e^{(\alpha^0 - \beta)t} - I) + (\alpha^0 - \beta)^{-1} \alpha_x e^{(\alpha^0 - \beta)t} \quad (59)$$

similarly we can get $\partial_y c_2^0(t)$.

■